

VARIATION OF DEFORMATION MECHANISMS WITHIN THE PROGRESSIVE–RETROGRESSIVE MYLONITIZATION CYCLE OF LIMESTONES: BRUNOVISTULIAN SEDIMENTARY COVER (THE VARISCAN OROGENY OF THE SOUTHEASTERN BOHEMIAN MASSIF)

PETR ŠPAČEK^{1*}, JIŘÍ KALVODA¹, EVA FRANČU² and ROSTISLAV MELICHAR¹

¹Department of Geology and Paleontology, Masaryk University, Kotlářská 2, 61137 Brno, Czech Republic; *vajgl@sci.muni.cz

²Czech Geological Survey, Leitnerova 22, 60200 Brno, Czech Republic

(Manuscript received December 7, 2000; accepted in revised form June 13, 2001)

Abstract: This study deals with the calcite mylonites of the Brunovistulian sedimentary cover developed in the frontal thrust area of the Moravian nappe units. The inhomogeneous structure of sedimentary protoliths allowed the analysis of the contrasting behaviour of calcite in matrix and porphyroclasts and the interpretation of microfabric evolution during deformation under low temperature conditions. Several stages of microfabric evolution characterizing progressive as well as retrogressive deformation are distinguished. Generally, the progressive phase of mylonitization is characterized by grain growth in the matrix and the grain size reduction of the porphyroclasts leading to a stress-induced equilibration of grain size. During the initial deformational stages the calcitic porphyroclasts deformed brittly and the strain was strongly localized into the ductile matrix. With continuing evolution the onset of the dynamic recrystallization of porphyroclasts occurred, which obviously preceded a significant grain growth in the matrix. With rising temperature during deformation, grain growth predominated after grain size homogenization was finished. The lack of effective dynamic recovery along the stages of the progressive low temperature phase of deformation is discussed. Core-and-mantle structures which are characteristic of the initial stages of progressive deformation carry microfabric features which document the dominance of grain boundary bulging and/or nucleation recrystallization. Formation of subgrains within the porphyroclasts is only a rarely observed feature which probably could not lead to significant grain size reduction. The higher effectiveness of nucleation and recrystallization via migration of grain boundaries compared to subgrain rotation mechanism could be a consequence of high fluid content. Large-scale thrusting within the Brunovistulian basement is shown by the juxtaposition of calcitic and quartzitic mylonites with deformational microstructures reflecting pronounced contrasts of deformational styles. Fully plastic vs. fully brittle behaviour of quartz represents the most pronounced indicator of different deformational conditions between the lower unit of the Svratka Dome and the other domains of the Brunovistulian basement. In the lower tectonic unit of the Svratka Dome the microstructures of calcite mylonites indicate stresses which were about four times lower than in the other two parts of the Brunovistulicum. Despite the deformational contrasts, the values of illite crystallinity measured do not show any spatial gradient which could be linked with the distribution of the contrasting deformational microstructures. The paleothermometric data which are available to date suggest maximum paleotemperatures of 250–300 °C for all three studied domains of the Brunovistulian basement and it is suggested that the difference of Variscan peak temperatures between the three compared domains of the basement was not higher than several dozens of °C. The observed deformational contrasts can thus be explained by an abrupt change of deformation mechanisms in both calcite and quartz at temperatures around 300 °C.

Key words: Eastern Variscan front, Brunovistulicum, inhomogeneous limestones, mylonitization, dynamic recrystallization, microstructures.

Introduction

Microfabric studies of strained homogeneous calcite aggregates have been described relatively frequently, both in nature (e.g. Dietrich & Song 1984; Heitzmann 1987; Burkhard 1990; Covey-Crump & Rutter 1989; Busch & Van der Pluijm 1995) and experiments (e.g. Schmid et al. 1977, 1980, 1987; Rutter 1974; Rutter et al. 1994; Walker et al. 1990). However, research into the mylonitization of inhomogeneous carbonates, which are the most abundant in nature, is rather sparse. Therefore we attempted to give a detailed study of the development of such inhomogeneous limestones in low-temperature (LT) deformational stages.

In the southeastern part of the Bohemian Massif, the tectonic contact of the allochthonous domain of Variscan orogen (the Moldanubian and Moravian nappe units) and the per-autochth-

onous pre-Variscan basement (the Brunovistulicum) is exposed (Matte et al. 1990). The Devonian and Lower Carboniferous carbonate-clastic sedimentary cover of the Brunovistulicum is strongly sheared in the thrust area under anchimorphic and very low-grade metamorphic conditions (Schulmann et al. 1991). Calcite mylonites from this highly deformed sedimentary sequence were studied along orogen-perpendicular profiles, which cross-cut the foot-wall of the Moravian nappe units and proximal parts of their foreland.

As the microstructure of sedimentary protoliths was generally inhomogeneous, the mylonites served as a suitable object for the comparison of the deformational behaviour of the matrix vs. the porphyroclasts within the given spectra of LT deformational conditions. The analysis of deformational microfabric allowed the interpretation of its evolution during the progressive transformation of limestones into mylonites and

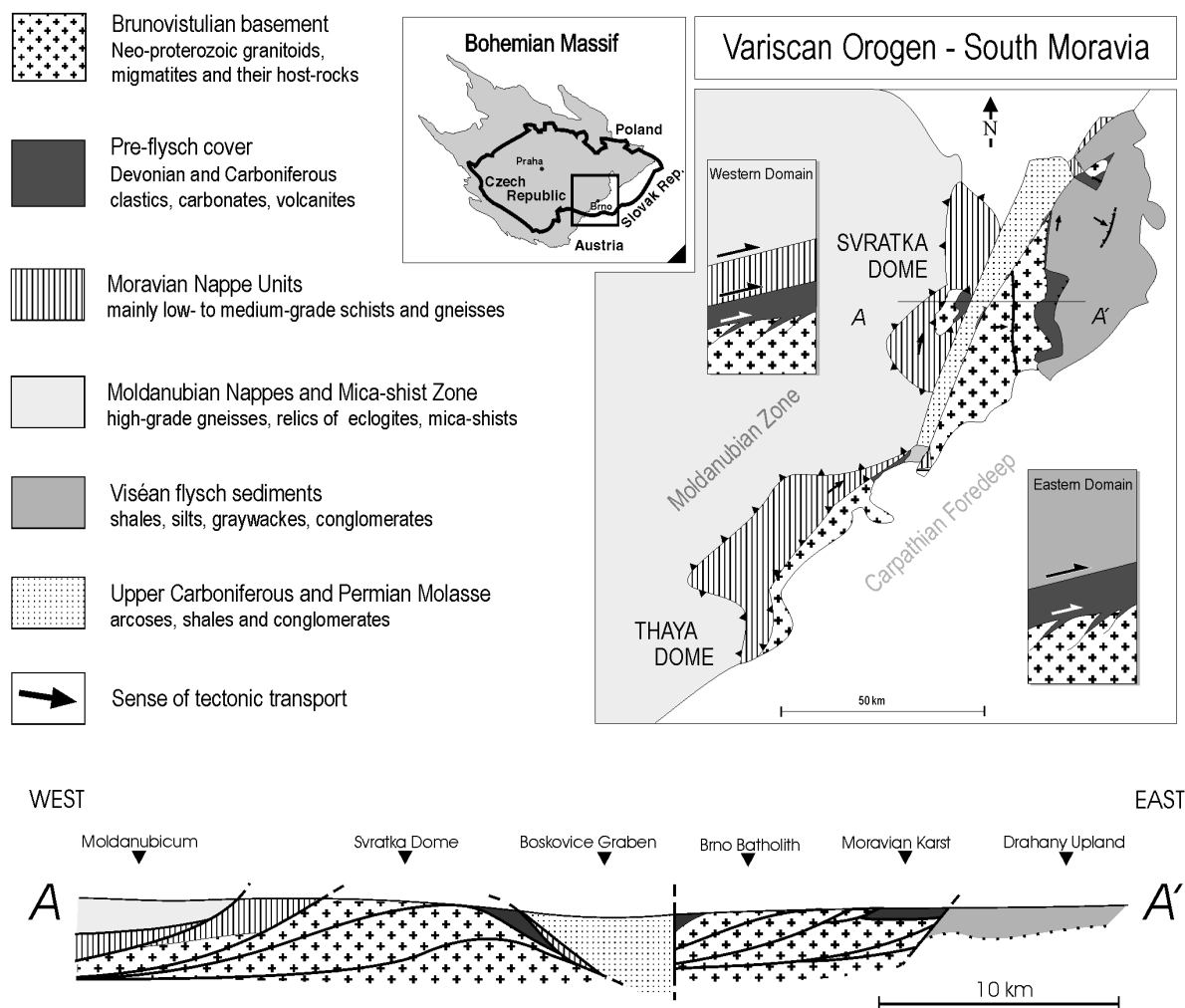


Fig. 1. Schematic map of the area studied and a conceptual profile through the main units of the collision zone.

during retrogressive degradation under decreasing temperatures. On the basis of the observed deformational microstructures it was possible to make a comparison between three domains of the Brunovistulicum in terms of dominant deformational regimes in calcite aggregates.

Geological settings

The Variscan assembly of the allochthonous units and the Brunovistulian basement within the eastern Bohemian Massif are related to the Devonian-Late Carboniferous dextral oblique collision of the Armorican terranes (Moldanubian and Saxothuringian Terrane) with the Brunovistulian Terrane — outer part of Laurussia (Matte et al. 1990; Kalvoda 1995, 2001). Three main units have been distinguished in the collisional zone: Moldanubicum (Suess 1912) with high grade Variscan metamorphism (Suess 1912, 1926; Cháb & Suk 1977), Moravian Zone (Suess 1912) with medium grade Variscan metamorphism (Suess 1912, 1926; Štípská & Schulmann 1995) and Brunovistulicum (Dudek 1980), in which the Variscan metamorphism is low-grade and occurs only in a close contact with the overlying tectonic units (Schulmann et al. 1991; Franců et al. 1999). According to some authors the

nappe units of the Moravian Zone were derived from the highest parts of the imbricated Brunovistulian basement (e.g. Fras 1983; Fritz & Neubauer 1993; Štípská & Schulmann 1995), as indicated mainly by similar radiometric ages of the Brunovistulian granitoids and sheared orthogneiss bodies of the Moravian nappes (van Bremen et al. 1982; Morauf & Jäger 1982).

The structure of the southern part of the collisional zone is well exposed in two incomplete tectonic windows: the Thaya Dome in the south and the Svratka Dome in the north (Fig. 1). A similar lithotectonic zonation has developed in both of them, as described, for example, by Schulmann et al. (1991, 1994) and Fritz & Neubauer (1993):

- 1 (bottom). Granitoids, metagranitoids and migmatites of the Brunovistulian Cadomian basement with their metasedimentary host rocks and Paleozoic sedimentary cover (Dudek 1980; Finger et al. 1989, 1995; Bosák 1980; Batík & Skoček 1981),
2. Moravian nappe units composed mostly of metasediments, pre-Variscan Bíteš orthogneiss and its metasedimentary host rocks (e.g. Schulmann et al. 1991),
3. Mica-schist zone with metasediments, amphibolites and orthogneiss bodies (Suess 1908),
- 4 (top). Moldanubian nappes with high-grade granulites, paragneisses, migmatites and relics of eclogites (Matějovská 1975; Jenček & Dudek 1971; Vrána et al. 1995).

Characteristic features of this sequence are inverted Barrovian metamorphic zoning, metamorphic foliation parallel with lithological boundaries and N to NE trending lineations subparallel to the axes of tight folds (Schulmann et al. 1991). In the upper units, E-W stretching lineations are common (Fritz & Neubauer 1993).

In the foreland of the Moravian and Moldanubian nappe units, the Brunovistulian basement is exposed in the Brno batholith and has been verified through many boreholes beneath the Paleozoic cover on the eastern slopes of the Bohemian Massif. In this eastern part of the collisional zone different lithotectonic zonation is developed:

1 (bottom). Cadomian granitoids of the Brunovistulicum with its metamorphosed host-rocks and Devonian-Lower Carboniferous pre-flysh sedimentary cover (e.g. Dudek 1980; Leichmann 1996; Hanzl & Melichar 1997; Finger et al. 2000; Dvořák 1995),

2. several km thick flysh sequence of Viséan age (Dvořák 1973; Rajlich 1990; Čížek & Tomek 1991).

The Viséan flysh sequence is strongly folded (e.g. Rajlich 1990) and Čížek & Tomek (1991) proved the existence of large-scale east-vergent thrusts imbricating both the flysh sequence and the Brunovistulian basement with its tectonized pre-flysh sedimentary cover. In this part of the orogen, the ductile deformation of the rocks is non-penetrative and thick zones of mylonitization occur only in close proximity to the Moravian nappes. Stretching lineation and associated kinematic indicators show top-to-the-NNE shearing (e.g. Bábek & Janoška 1997). In general, the degree of Variscan deformation and metamorphism is very low and further decreases to the east where Paleozoic sequences rest autochthonously on the Brunovistulian basement.

Within the Brunovistulian basement, two parts with different development during the Variscan orogenesis can thus be distinguished. The first is in the westernmost part with the Moravian nappes in the hanging wall and the second in the eastern part is covered by Viséan flysch nappes. The boundary of these two sections is covered by Westphalian-Autunian sediments of the Boskovice Graben. The exact meaning of the tectonic contact of units beneath the sedimentary infill of the graben is still not well understood.

For the tectonic evolution of the collisional zone the forward thrust propagation model was suggested by Schulmann et al. (1991), Fritz & Neubauer (1993) and Fritz et al. (1996). The thrusting began under HT conditions and continued during gradual cooling to LT conditions. The deformation regimes were changing continuously from top-to-the-N shear through top-to-the-E shear to E-W coaxial extension. The simultaneous activity of non-coaxial shearing in the lower units and the coaxial extension in the upper units has been assumed. This model explains the complex structural evolution and systematic decrease of isotopic ages of metamorphism from the uppermost tectonic to the lowest tectonic levels.

Analytical methods

The transformations of the primary structures of inhomogeneous carbonate sediments into a deformation fabric of carbonate mylonites were analysed. Dozens of samples were collect-

ed in both parts of the basement — from the foot-wall of Moravian nappe unit in the western part and from the foreland of the Moravian nappes in the eastern part of the basement (Figs. 1 and 6). The key steps in the analytical procedure, which should have provided data for the interpretation of deformation mechanisms and conditions, were:

- 1) the description and quantification of the optical deformation microstructures and lattice preferred orientations (LPOs);
- 2) the correlation of the microfabric with the temperatures of deformation.

Microstructures

Thin and ultra-thin (<10 µm) sections were prepared from oriented samples cut parallel to XZ and ZY planes of finite strain and were examined under optical and SEM microscopes. Grain-shape analyses of the coarse-grained domains were carried out using a polarizing microscope-digital camera-computer arrangement. Images of the thin sections were captured in two or three different polarizer/analyzer positions in order to identify the maximum number of grain-boundaries (Burkhard 1990). The two or three images obtained were projected on a horizontally oriented screen in a slideshow mode and the grain boundary networks were then produced by manually outlining the grains onto transparent foil. For the SEM morphological analyses of the fine-grained aggregates, polished XZ and XY slabs of the selected samples were etched in a 1% hydrochloric acid solution for 10 seconds and coated with gold-film. Secondary electron photomicrographs were obtained from 30–50° tilted samples after tilt-correction.

Quantitative processing of the grain boundary networks was carried out using *ImageTool 2.0* software. In this paper, only the grain size parameter is used for the characterization of microstructures. The grain size (D) is defined as the diameter of a circle with the same area as the grain being measured, that is

$$D = \sqrt{4 \times \text{grain area} / \pi}.$$

Such a definition of grain size gives the most realistic values which are independent of grain shape. For stress calculations we used the Rutter paleopiezometer (Rutter 1995) calculated for the grain boundary migration (GBM) recrystallization mechanism:

$$\log \sigma = 2.22 + 0.37 \log d - 0.30 (\log d)^2,$$

where σ is the differential stress and d is the grain size, and the median values of grain size were used as suggested by Ranalli (1984).

The content of dolomite and other secondary phases was examined with an electron microprobe in selected samples in order to assess their potential influence on the deformational processes.

The stretch (S = original length/finite length of the deformed object) was measured at pressure fringes, deformed peloids and ooids, boudinaged clasts and other strain-markers in order to demonstrate the strain magnitude of the distinguished microstructural types.

Lattice Preferred Orientations (LPO)

If the evolution of the mylonites was to be reconstructed, it was necessary to determine the mechanisms operative during the deformation. Therefore the LPO were measured. Their in-

tensity is related to the magnitude of the intracrystalline deformational mechanisms and their ratio to the other mechanisms of deformation (e.g. Casey & McGrew 1999). X-ray diffraction texture analysis was used for the comparison of the fabric geometries and intensities of the distinguished microstructural types. The measurements were carried out in the laboratory of Military Technical Institute of Protection in Brno, using a Siemens D-500 texture goniometer. Textures were measured using reflection geometry on thin slabs of the rock which had been cut parallel to the macroscopic foliation (XY plane). Filtered $\text{CuK}\alpha_{1+2}$ rays were used and maximum tilt was 80° . The data were further tilt-corrected, using a tilt scan on a powder sample and processed with *popLA* software (Kallend et al. 1991).

Preliminary results have shown that the LPO patterns of all samples are very similar and that it was not necessary to calculate orientation distribution functions. The LPO intensities of the samples measured were compared in the incomplete ($\Phi = 0\text{--}80^\circ$) pole figures of (018) planes (*e*-poles).

Additionally, crystallographic orientations of the coarse grains were measured in several thin sections using optical polarizing microscope with a U-stage. This “semi-domainal” LPO analysis allowed the LPO of the porphyroclasts and that of the whole samples to be measured separately.

Paleothermometry

The illite crystallinity of clay fractions from shales associated with the mylonitized limestones was measured in order to estimate the maximum reached paleotemperatures. Clay-size material was separated from 8 rock samples after removing the cements such as carbonates, organic matter and iron oxides (Jackson 1975). Clay fraction $< 2\ \mu\text{m}$ was collected by centrifugation for determination of illite crystallinity. Oriented slides were analysed both air-dry and after vapour glycolation using X-ray diffractometer Philips PW 1830 (generator) and PW 3020 (goniometer) with 0.02° step from 2 to $50^\circ 2\theta$. Illite crystallinity index (IC) was measured as peak width in $\Delta 2\theta$ at half maximum (PWHM) of the (001) basal reflection of illite (Kübler 1967) using background stripping and peak-fitting. The results were calibrated to international standards (Warr & Rice 1994).

Microstructures and their interpretations

The results of microfabric analyses allow several basic groups of (proto-)mylonites with similar features to be distinguished. In the following discussion, these groups of microstructures will be identified with the letters A–E. The interpreted mechanisms of deformation are shown in a schematic diagram in Fig. 3.

Microstructures A. Weakly deformed protoliths

Rocks of this type retain their original inhomogeneous structure and the sedimentary attributes of their protoliths. The most typical composition includes a micritic matrix ($d \sim 4\ \mu\text{m}$) and a wide-ranging assemblage of various parts of fossil organisms, which together with boudinaged veins and other con-

stituents composed of sparite, will be referred to as “porphyroclasts”.

Strain markers, for example, the calcite-filled pressure fringes around quartz clasts and deformed peloids, indicate that matrix suffered substantial strains with minimum stretch values up to $S = 4.5$. In spite of this high degree of strain, the micrite in the matrix does not exhibit substantial microstructural changes.

The coarse-grained porphyroclasts are not substantially internally strained and figure as rigid bodies passively flowing in a ductile environment. Locally, book-shelf fracturing, microboudinage, twinning and only slight undulose extinction within the coarse grains can be observed in the samples with higher finite strains or with the load-bearing framework of coarse grains. The distribution of the *c*-axes measured in porphyroclasts is random to strong with a single maximum near the pole to the foliation, depending on the strain magnitude (not shown in the figure, in strongly deformed types the *c*-axes distribution is very similar to that in Fig. 2d). Bulk (whole sample) X-ray LPO is much weaker, increasing with the higher volume of the clasts (Fig. 2a).

Fabric development of this microstructure took place in a semi-ductile regime. Strain partitioning due to grain size inhomogeneity, with preferential localization into fine-grained matrix, is characteristic. For the matrix, the interpreted dominant mechanism of the deformation is grain boundary sliding (GBS) with accommodation by diffusion transfer at grain boundaries. The main arguments for GBS are negligible microstructural changes in spite of high strains and the weak LPO. The high water content in the limestones during deformation is indicated by frequent pressure fringes and stylolites in the micrite. It is very likely that the fluids have played an important role in the diffusive matter-interchange between the grains and could thus have caused a substantial weakening of the matrix. During the deformation, the strength of coarse grained porphyroclasts was much higher than that of the fine-grained matrix (compare Fig. 7a). Local high stress conditions resulted in brittle fracturing, twinning and incipient intracrystalline slip within the porphyroclasts.

Microstructures B. Protomylonites

A mantled porphyroclasts/matrix structure is characteristic for this group (Fig. 7b). Core-and-mantle structure grains are free of clay minerals and in most cases can be easily distinguished from the matrix which appears darker under transmitted light. The bulging of the grain boundaries and the formation of oval-shape recrystallized grains (Fig. 7c) takes place preferentially at twin lamellae and boundaries of clasts.

This type of microstructure is interpreted as a result of grain boundary bulging (GBB) or nucleation recrystallization (Drury & Urai 1990; Mercier et al. 1977). High aspect ratios of the porphyroclasts were generated mainly by the superposition of GBM on the twin lamellae (Fig. 7b). Within the matrix, non-distinctive grain growth up to $d < 10\ \mu\text{m}$ also indicates the incipient activity of grain boundary migration. The formation of subgrains and rotation recrystallization are less pronounced and do not lead to significant reduction in grain size. Despite the occurrence of mantled porphyroclasts, which one is tempted to interpret as the product of subgrain rotation, the lack of recovery in the grains suggests the dominance of the GBB

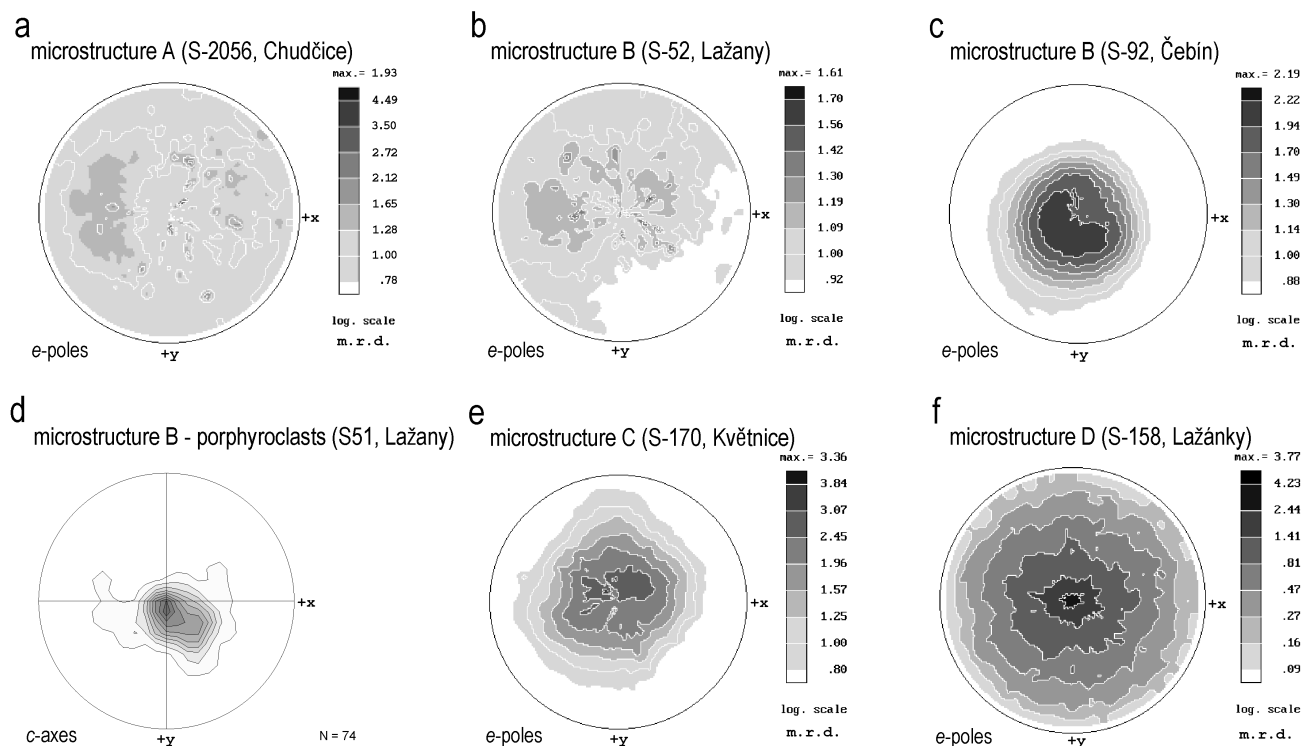


Fig. 2. Sample pole figures of *e*-planes and *c*-axes of the main microstructural types. All data are projected to the plane of foliation in equal-area projection, lower hemisphere. **a–c, e, f** — X-ray diffraction data in incomplete pole figures; intensities are expressed as multiples of a random distribution (m.r.d.). **d** — *c*-axes distribution of porphyroclasts in microstructure B. Contours at 0, 2, 4, 6, 8, 10, 12, 14, 16 and 18 %. Notice the strong LPO of porphyroclasts vs. weak LPO of whole sample in the microstructural types B and the increasing intensity of the preferred orientation from Type B to Type D with relatively constant distribution geometry. The patchy pattern of the distribution is due to the high content of large grains in the samples.

	ca. 250°C		ca. 300°C		
microstructure	A	B	C	D	E
matrix	GBS (+fluid transfer)		GBS?+DG+GBM		
porphyroclasts	cataclasis, twinning	DG+GBB+nucl.	DG+SGR+GBM		
		BPT of porphyroclasts		grain-size homogenization	

Fig. 3. The interpreted dominant deformational mechanisms operative in the distinguished stages of mylonitized limestones. **GBS** — grain boundary sliding, **GBB** — grain boundary bulging, **DG** — dislocation glide, **GBM** — grain boundary migration, **SGR** — subgrain rotation recrystallization, **nucl.** — nucleation, **BPT** — brittle-plastic transition.

and/or nucleation mechanisms of recrystallization. The recrystallized grains produced by grain size reduction of the porphyroclasts are usually larger in size than those resulting from the grain growth of the matrix micrite (Table 1). This discrepancy can be explained by the low rate of GBM in the matrix grains as a result of their low level of internal strain and/or the inhibitory effect of the secondary phase (Olgaard & Evans 1988). The LPO of these types of protomylonites have features similar to that of the microstructures A: a strong single maximum of the *c*-axes close to the pole of foliation in the porphyroclasts, which is weakened in the LPO of the whole sample (Fig. 2b,c,d). The activity of GBS is likely to have persisted in both the matrix and the domains of recrystallized grains as indicated by the lack of microstructural change in spite of strong

deformation of the fine-grained domains. Boudinaged bio-clasts indicate minimum stretch values of $S = 6.1$.

Microstructures C. Mylonites

These types of rocks are composed of a relatively coarse-grained matrix ($d = 20\text{--}50\ \mu\text{m}$) with relict porphyroclasts. Pressure fringes indicate minimum stretch values of $S = 6.0$. Grain aspect ratios vary between 1.5 and 4. All the grains of the matrix and the porphyroclasts are optically strain free, grain boundaries are almost straight, slightly curved or bulbous. Twin lamellae are rare, straight and were probably produced during cooling due to high thermoelastic anisotropy of calcite (Rosenholtz & Smith 1949). The LPO is similar both for matrix and porphyroclasts, showing single maximum of *e*-poles (and *c*-axes respectively) close to the pole of foliation (Fig. 2e). Because the grains lack undulose extinction and a subgrain microstructure and the grain boundaries are frequently bulbous, we attribute the finite microstructure to GBM-dominant recrystallization. Nevertheless, twinning and/or dislocation glide are also likely to have played a substantial role during earlier phases of the deformation as indicated by high aspect ratios and straight boundaries of the grains and the enhanced intensity of LPO.

Locally, sharply terminated prolate lens-shaped domains are developed in these types of mylonites, representing strained stems of *Amphipora* sp. These domains are composed of rela-

Table 1: Grain size values and calculated paleostresses of selected typical samples of the calcite mylonites studied. In some domains, stresses were not calculated for the reasons expressed by abbreviations: *sp* — high content of secondary phase (possible inhibition of grain growth), *nu* — not well understood mechanisms of origin (inhomogeneous tectonofacies with ambivalent characteristics), *ss* — non-recrystallized primary sedimentary structures, *crm* — combination of recrystallization mechanisms.

tectonic domain	microstructure	sample no., locality	microstructural domain (and responsive deformation phase)	d (μm, median)	σ _{diff.} (MPa)
eastern	B	s88b, Čebín	matrix	4.0	ss
eastern	B	s88b, Čebín	recrystallized grain mantles (peak metamorphism)	6.2	211
eastern	B	s90-1, Čebín	matrix	5.0	ss
eastern	B	s90-1, Čebín	recrystallized grain mantles (peak metamorphism)	8.2	203
eastern	B	s51a, Lažany	matrix	5.41	ss
eastern	B	s51a, Lažany	recrystallized grain mantles (peak metamorphism)	6.7	209
eastern	B	s188, Šebetov	recrystallized grain mantles (peak metamorphism)	8.0	204
western	B	s45-1, Kadov	matrix	4.3	ss
western	B	s45-1, Kadov	recrystallized grain mantles (peak metamorphism)	7.2	207
western	C	s170, Květnice	fine grained domains	12.3	nu
western	C	s170, Květnice	coarse grained domains	26.9	nu
western	C	s 239, Vohančice	fine grained domains	19.6	nu
western	C	s 239, Vohančice	coarse grained domains	27.3	nu
western	D	s166-1, Dranč	coarse grained domains (peak metamorphism)	100.5	57
western	D	s171, Lažánky	fine grained domains	30.6	sp
western	D	s171, Lažánky	coarse grained domains (peak metamorphism)	115.6	51
western	D	s158, Lažánky	coarse grained domains (peak metamorphism)	89.4	63
western	D	s151, Dřínová	coarse grained domains (peak metamorphism)	102.4	56
western	D	s157, Vohančice	coarse grained domains (peak metamorphism)	111.5	52
western	E	s157, Vohančice	fine grained domains (incipient retrogression)	38.9	crm
western	E	s157, Vohančice	fine grained domains (advanced retrogression)	24.4	crm

tively coarse grained calcite aggregates of equant, strain free grains with slightly curved boundaries.

Microstructures D. Coarse grained marbles

In the most mature mylonites mesoscopic indicators (sheath folds, boudinaged clusters of dolomite) suggest stretch values of $S > 10$. In these types characteristic homogeneous domains are developed with a uniform grain size which varies with the volume of the dispersed phyllosilicates and dolomite (Table 1). Porphyroclasts composed of calcite are absent. In the domains with a small amount of secondary phases, the grain size usually reaches 100–120 μm. All grains are strain free, having slightly curved to lobate boundaries. Grain aspect ratios are usually > 2.5 and occasionally domains with equant coarse grains with grain boundaries meeting in 100–140° triple junctions can be observed (Fig. 7d). The *c*-axes distribution pattern shows a strong single maximum close to the pole of foliation (Fig. 2f). Rare twin lamellae are straight, and were probably produced during cooling. The microstructural features of these types suggest the dominance of GBM recrystallization mechanism. However, strong LPO indicates substantial activity of intracrystalline deformation during the evolution of these types, whose microstructures could have been overprinted in the latest phases of the deformation.

Microstructures E. Retrogressively deformed marbles

In some areas, grain size reduction of the coarse grains occurs within D types and narrow shear zones are developed affecting coarse-grained aggregates of microstructure D (Table 1). The old grains are polygonized into subgrains and newly formed grains usually have a crystallographic orientation very close to that of their host grains (Fig. 7e). As the grain boundaries of the recrystallized grains are interpenetrating and bulbous, we suggest that the grain size reduction is an effect of the combination of both subgrain rotation and GBM mecha-

nisms. These structures are attributed to the onset of retrogressive deformation during incipient cooling. Further low temperature deformation of some domains generated strong twinning and undulose extinction of the coarse grains.

Paleothermometry

Illite crystallinity was measured in clay fractions of eight samples from both the Svratka and Thaya Domes and western margin of the Brno batholith. Two samples were excluded from further processing because of their high content of expandable smectite and chlorite.

The values of illite crystallinity index (IC) range from 0.20 to 0.35° $\Delta 2\theta$ (Table 2) and indicate higher part of very low-grade metamorphic (VLGM) conditions with probable maximum paleotemperatures of 250–320 °C (calibration after Frey & Robinson 2000). The thermal alteration is more advanced than in most Paleozoic rocks of the Drahaný Upland which show mainly lower VLGM conditions (Franců et al. 1999). The results of IC thermometry are consistent with the data of Bosák (1984) who analysed the degree of kerogen graphitization in dark carbonate rocks of the lower units of the Svratka Dome and of the western margin of the Brno batholith. He concluded that in most samples from the Svratka Dome the maximum temperature did not exceed 300 °C and that the grade of thermal alteration of organic matter was considerably lower in the carbonates of the Brno batholith's western margin. Similar conclusions were made recently by Ulrich (2000) who analysed the carbon and oxygen isotopic composition of six carbonate samples from two localities in the lowermost unit of the Svratka Dome. Using the graphite-calcite thermometer and calibration of Covey-Crump & Rutter (1989) he stated that the maximum temperatures in the graphite-rich marbles did not exceed 300 °C for a longer period of time. In the limestones of the Brno batholith's western margin paleotemperatures of 250–300 °C are indicated by the degree of conodont

Table 2: Illite crystallinity values of clay fractions from shales associated with the mylonitized limestones. **BB** — Brno batholith's western margin, **TD** — lower tectonic unit of the Thaya Dome, **SD** — lower tectonic unit of the Svratka Dome. (*) — associated tectonofacies are marked with capital letters in parentheses.

tectonic domain*	lithology	locality	IC ($\Delta^{\circ}2\theta$)
BB (A)	clayey limestone	Újezd u B. (s168)	0.30
BB (A)	shale	Újezd u B. (s168b)	0.28
BB (B)	clayey limestone	Šebetov (s111)	0.25
BB (A)	shale	Chudčice (s161)	0.20
TD (B)	shale	Skalice (s221)	0.35
SD (D)	shale	Lažánky (s237)	0.24

alteration. The black colour of the conodonts without the tones of brown corresponds to conodont colour alteration index (CAI) 5–5.5 (see Frey & Robinson 2000 for calibration).

Indirectly, and with limited reliability, the available paleothermometric data which are summarized in Table 3 can be supported by the features of deformation microstructures observed in quartz. In metamorphosed basement crystalline rocks and Devonian conglomerates and sandstones of the lower tectonic unit of the Svratka Dome, quartz aggregates carry clusters of recrystallized quartz grains with a similar *c*-axis orientation and intensely sutured grain boundaries. Well-developed low-angle boundaries and subgrains inside relic old grains are commonly found (Fig. 7g). This fabric is indicative of deformation by dislocation creep with recovery, subgrain rotation recrystallization and grain boundary migration being operative. The features of the microstructure thus correspond to the fully plastic deformation regime 3 of Hirth & Tullis (1992). After Stöckhert et al. (1999), the steady-state medium stress dislocation creep of quartz in the fully plastic regime can only be effective at temperatures above the closure temperature for K-Ar and Rb-Sr systems of biotite, that is above ca. 310 ± 30 °C. In contrast, in the eastern tectonic domain, quartz is brittly deformed, lacking any traces of intracrystalline slip (Fig. 7h). We consider similar pressure of fluids during the deformation of the quartz aggregates in both units. It seems to be a reasonable assumption that in the eastern part of the Brunovistulian basement (external part of the orogen) the brittle quartz was not deformed at higher strain rates than the plastic quartz in the lower tectonic units of the Svratka Dome (more internal part of the orogen). Assuming this, the observed deformational microstructures of quartz indicate that in the

eastern part of the Brunovistulian basement (Brno batholith's western margin), the deformation was taking place under temperatures which were probably lower than 310 ± 30 °C.

The lack of significant IC differences between the compared domains of the Brunovistulian basement (Table 3) suggests that the metamorphic transformation of smectite into illite reached similar stages in the studied rocks of the Brno batholith's western margin, the Thaya Dome and the Svratka Dome and that the paleotemperature differences are below the detection limit of the IC paleothermometer.

Considering potential errors of the paleothermometers and the variation of the IC values measured, it can be stated that the maximum paleotemperatures under which the studied rocks were deformed probably lie between 250 and 300 °C (Table 3). As was discussed above, the deformational features of both quartz and calcite indicate that in the Brno batholith and the lower unit of the Thaya Dome the maximum paleotemperatures were somewhat lower than in the lower unit of the Svratka Dome. However, the paleothermometric data constrain the maximum difference of Variscan peak temperatures between the three compared domains of the basement to several dozens of °C only (see Table 3).

The development of mylonitic stages

The sequence of microstructures A–E which has been distinguished above can be seen as a succession of frozen-in stages within the process of the deformational and metamorphic transformation of sediments. Several facts justify such an opinion: the analogous lithostratigraphic position of calcite mylonites, their overlapping biostratigraphic ranges and the mutual transitions of microstructural stages. A schematic diagram of the model is presented in Fig. 4. It is necessary to stress the fact that unquestionable primary sedimentary markers — fossil organisms — are common within the microstructures A, B and C. Microprobe analyses revealed a calcitic composition of the fossils. This is the main argument for interpreting the A–D sequence as a product of progressive mylonitization under increasing metamorphic conditions. During the retrogressive deformation phases, the fine-grained matrix of Type C was probably reworked again, but a significant change in the microstructure did not occur. The Type C microstructures never acquired the features of D types during its

Table 3: Table of paleothermometric data of the studied area which are collected from the available literature.

Brno batholith's western margin	Lower tect. unit of the Thaya Dome	Lower tect. unit of the Svratka Dome
—	graphite/calcite thermometer (Ulrich 2001 with calibration after Covey-Crump & Rutter 1989)	—
—	CAI (Špaček 2001, calibration after Frey & Robinson 1999)	max. 300 °C
>250 °C	—	—
—	graphitization of kerogen (Bosák 1984)	—
<300 °C	<300 °C	max. 300 °C
250–320 °C	illite crystallinity (this work, calibration after Frey & Robinson 1999)	250–320 °C
—	dynamic recrystallization of calcite (this work, after Burkhard 1990)	—
min. 250 °C	min. 250 °C	>250 °C
—	plastic deformation of quartz (this work, after Stöckhert et al. 1999)	—
—	—	>310±30 °C

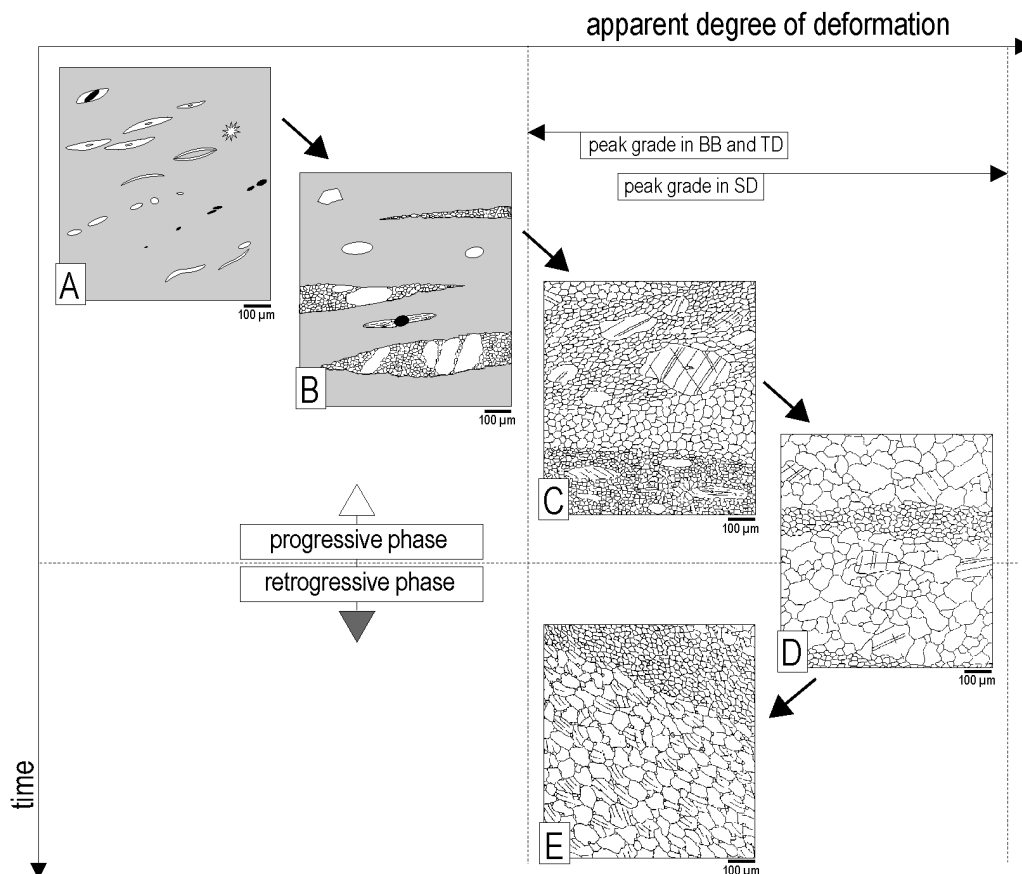


Fig. 4. Schematic diagram of microfabric development in mylonitized sequence of limestones. Notice the different peak grades reached in the lower tectonic unit of the Svatka Dome and the other two domains of the Brunovistulian basement. Objects in diagrams: **black** — quartz, **gray** — micrite and microsparite, **white** — coarse-grained calcite. **BB** — Brno batholith's western margin, **TD** — lower tectonic unit of the Thaya Dome, **SD** — lower tectonic unit of the Svatka Dome.

evolution. It was never fully homogenized and primary sedimentary structures were not completely destroyed. Thus, only the phase during which the microstructures E were produced is interpreted as retrogressive. Generally, the progressive phase of mylonitization is characterized by the grain growth of the matrix and a grain size reduction of the clasts leading to a stress-determined equilibrium of the grain size. With rising temperature during deformation, the homogenization of grain size was finished and grain growth predominated. In retrogressive phase, grain size reduction occurred due to a decreasing temperature and increasing stress.

Mechanisms of recrystallization

One of the most surprising features one can observe in the mylonitized sequence of carbonates studied is the dominance of GBB and the lack of effective dynamic recovery within the microstructures of the progressive low temperature phase of deformation.

Recovery represents the process of ordering the lattice defects, originated during intracrystalline slip, into subgrain boundaries which leads to a decrease in the internal strain energy of the crystal. When dislocations are continuously added to subgrain boundaries, the misorientation of the subgrains increases and new grains are formed. This process of new grains

formation is referred to as subgrain rotation recrystallization (SGR) and produces diagnostic core-and-mantle structures with (sub-)grains increasingly misoriented towards the external parts of mantle (Guillopé & Poirier 1979; Lloyd & Freeman 1994). If the temperature is high enough to enable ordering of the lattice defects, continuous recovery-accommodated dislocation creep can operate. However, when the temperature is too low, recovery cannot keep pace with the tangling of the dislocations during intracrystalline slip, newly formed dislocations cannot move and strain hardening of the lattice occurs (e.g. White 1977).

In our study, small ($d \sim 8 \mu\text{m}$) recrystallized grains of the mantled porphyroclasts in high stress mylonites B do not show any optical filiation to the host grains and their shape indicates the activity of GBB and/or nucleation (Fig. 7b,c). Although ultra-thin sections were used for the observation of microstructures, the formation of small-sized subgrains within the coarse grains was found only sporadically.

We therefore explain the recrystallization of the clasts in microstructures B as the product of a GBB-dominant process. Our observations lead us to the conclusion that during the progressive, low temperature deformation of the limestones studied, SGR was not capable of reducing the coarse grains into a steady-state size. Recovery and SGR produced only relatively large (sub-)grains which must have been further reduced by more effective GBB.

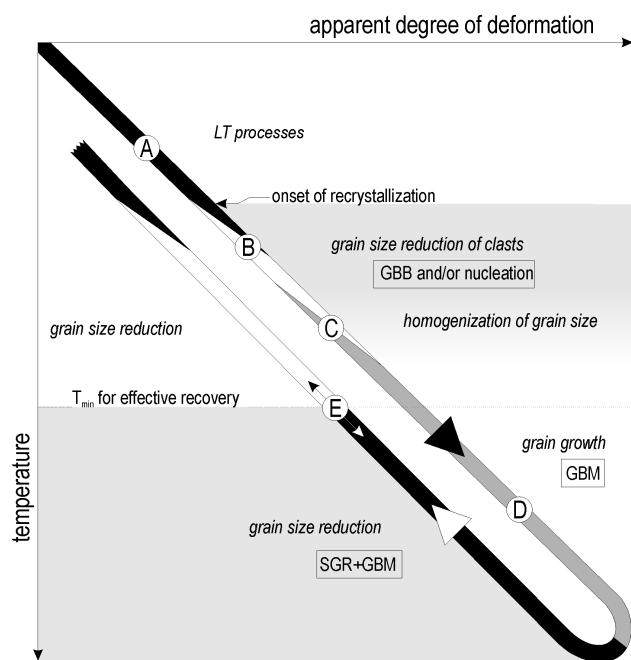


Fig. 5. The suggested model of recrystallization mechanisms in a complete deformation path of mylonitized limestones. Individual microstructures are marked with capital letters A–E. See text for explanations.

A suggested model of recrystallization development is shown in the Fig. 5. According to Lloyd & Freeman (1994), the velocity of grain boundary migration processes is determined by the relative crystallographic characteristics of adjacent grains, the driving forces, temperature and the structure of the boundary. Driving forces include mainly lattice defects, elastic energy and grain-boundary energy, and always lead to a decrease in internal strain energy. In our case, as the SGR did not lead to sufficient grain size reduction, each increment of continuing deformation raised the internal strain of the large grains and could accelerate the grain boundary bulging. Hippert & Egydio-Silva (1996) presented arguments for the activity of solution-precipitation process during the deformation of quartz which can be concurrent with solid state recrystallization. Thus the high content of water in the system, which is indicated by frequent markers of solution transfer, probably also significantly increased the GBB or nucleation rate (compare also with Tullis & Yund 1982). The facilitating of grain boundary migration resulting from a high water content would explain the contradiction of our model to observations of some other authors who suggest that SGR is more effective than GBB under lower temperatures (Schmid et al. 1987). The recrystallization mechanisms of calcite in LT conditions could be analogous to those of quartz, in which grain boundary migration-dominant structures have even been described for dry samples (Hirth & Tullis 1992).

Deformational contrasts and the imbrication of the Brunovistulicum

It has been demonstrated by many authors that inverse proportionality between stress and recrystallized grain size exists

(e.g. Twiss 1977; Kohlstedt & Weathers 1980). Thus, under a constant strain rate, the increase in recrystallized grain size is due to a decrease in material strength. Analogously, grain size distribution within a mylonitized sequence can be viewed as the result of metamorphic grade (i.e. temperature) variation. We therefore attempted to assess the differences between the deformation grade of the two domains of the deformed Brunovistulian basement. The most effective and reliable method of relative paleostress estimation seems to be the comparative measurement of grain size in the peak grade microstructures of individual tectonic domains. Uniform recrystallized grain size within broad domains justifies the presumption of steady state creep (e.g. Twiss 1977; Michibayashi 1993). Facies with small-scale grain size variations were not taken into account in the paleostress calculations. It was assumed that the coarsest recrystallized grain size within the defined groups of microstructures represents the peak metamorphic conditions. In many coarse grained domains of facies D, the lack of anneal-

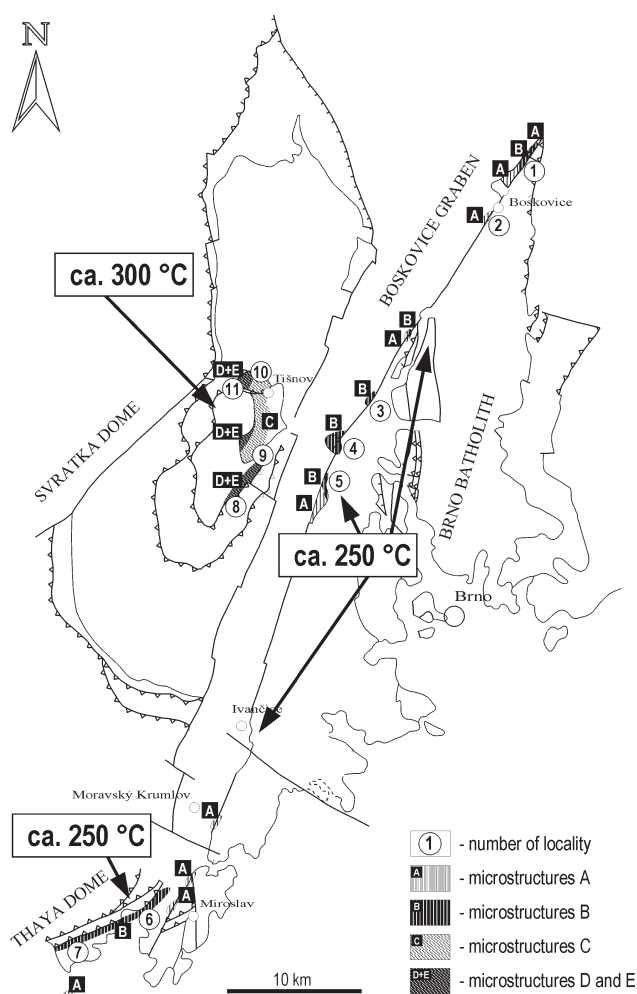


Fig. 6. Simplified sketch of the studied area showing the distribution of distinguished microstructural types. Circles with numbers indicate sampled localities which are referred to in the tables and figures. 1 — Šebetov (s111), 2 — Újezd u Boskovic (s168, s168b), 3 — Lažany (s51a), 4 — Čebín (s88b, s90-1), 5 — Chudčice (s2056, s161), 6 — Kadov (s45-1), 7 — Skalce (s221), 8 — Lažánky (s171, s158, s237), 9 — Vohančice (s157, s239), 10 — Květnice (s170), 11 — Dřínová (s151) and Dranč (s166-1).

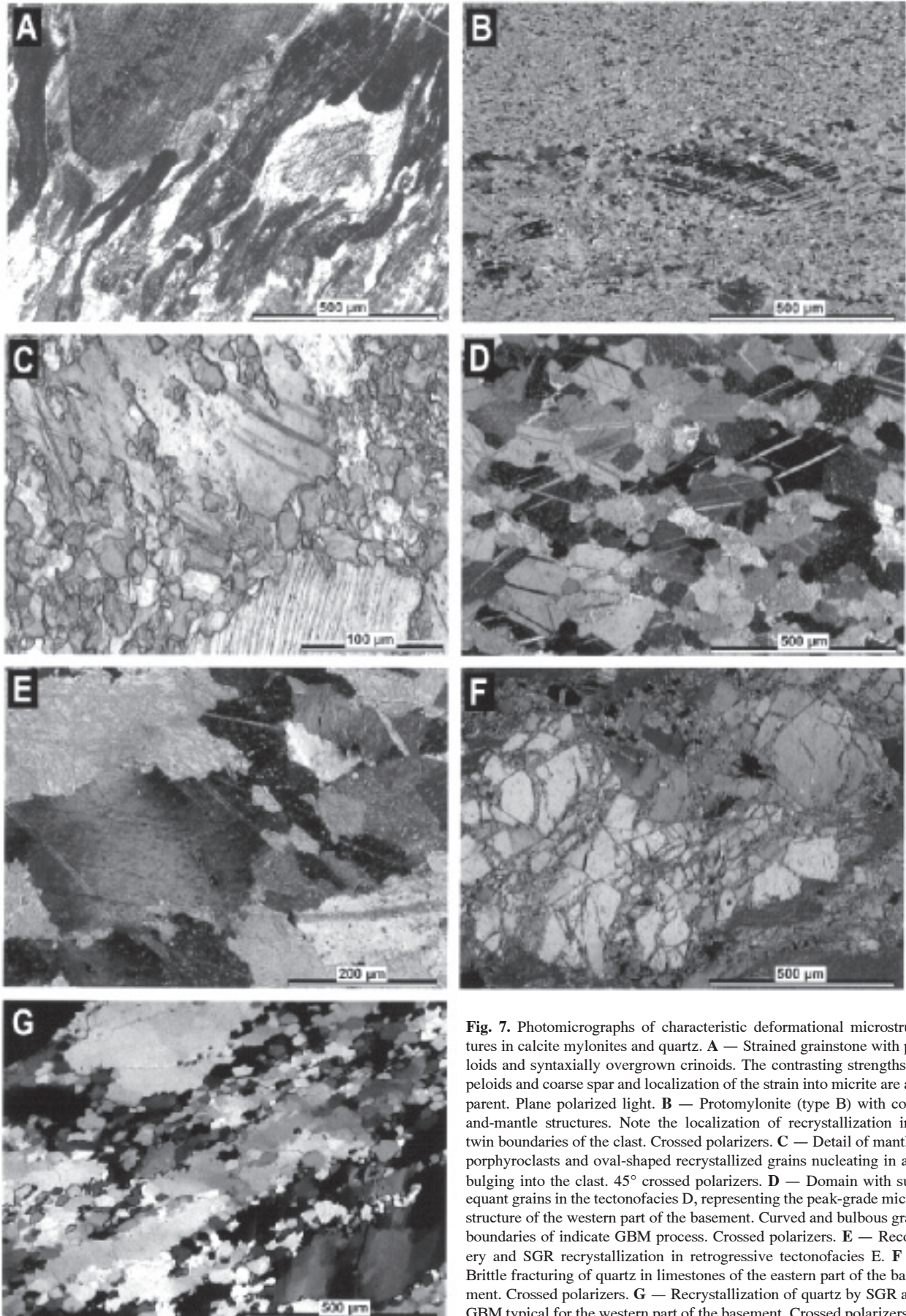


Fig. 7. Photomicrographs of characteristic deformational microstructures in calcite mylonites and quartz. **A** — Strained grainstone with peloids and syntaxially overgrown crinoids. The contrasting strengths of peloids and coarse spar and localization of the strain into micrite are apparent. Plane polarized light. **B** — Protomylonite (type B) with core-and-mantle structures. Note the localization of recrystallization into twin boundaries of the clast. Crossed polarizers. **C** — Detail of mantled porphyroclasts and oval-shaped recrystallized grains nucleating in and bulging into the clast. 45° crossed polarizers. **D** — Domain with subequant grains in the tectonofacies D, representing the peak-grade microstructure of the western part of the basement. Curved and bulbous grain boundaries indicate GBM process. Crossed polarizers. **E** — Recovery and SGR recrystallization in retrogressive tectonofacies E. **F** — Brittle fracturing of quartz in limestones of the eastern part of the basement. Crossed polarizers. **G** — Recrystallization of quartz by SGR and GBM typical for the western part of the basement. Crossed polarizers.

ing is evidenced with the shape of the grain boundaries, internal strain and polygonization of the grains. It can be stated that after reaching peak temperatures and the localization of the retrogressive deformation into narrow zones, no substantial grain growth took place in the domains which are now coarse grained. The stress calculations thus should not be affected by static recrystallization. In Table 1, the calculated paleostresses are given for several typical samples, using the Rutter paleopiezometer (Rutter 1995) for the GBM recrystallization mechanism.

If we compare the stress values of the facies B and D, which represent the peak metamorphic conditions in the eastern and western parts of the Brunovistulian basement respectively, we can see a significant difference. Stresses four times lower in the lower tectonic unit of the Svratka Dome than in the other two parts of the Brunovistulicum are in accordance with the observed deformation regimes of quartz. As the three compared parts of the Brunovistulian basement are eroded to a similar lithostratigraphic level, the tectonic juxtaposition of the contrasting facies must have occurred during late tectonic phases. The main contrasts however, are not seen between the two parts of the Brunovistulicum with different tectonostratigraphic zonation, which were defined above, but they lie between the lower tectonic unit of the Svratka Dome and the other two domains of the Brunovistulicum — the Brno batholith's western margin and the lower tectonic unit of the Thaya Dome (Fig. 6).

Summary and concluding remarks

The analysis of the mylonites assembly developed within the major thrust system of the Central European Variscan orogeny revealed several characteristic features:

- 1) A lack of effective dynamic recovery within the progressive low temperature phase of deformation. Microstructural features of core-and-mantle structures developed in calcite protomylonites provided evidence of GBB-dominance of the recrystallization process. In this phase, the SGR mechanism produced only relatively large grains, which must have been further reduced by GBB and/or nucleation. Recovery was effective only during grain size reduction in the retrogressive phase. This can be explained with a higher rate of GBB under lower temperatures, which could have been increased as a result of a high fluid content.

- 2) The onset of grain size reduction of porphyroclasts prior to distinct grain growth in matrix.

During the incipient mylonitization of inhomogeneous micritic limestones, the porphyroclasts and matrix display contrasting rheological behaviour and strong strain localization into a superplastic matrix occurs. At a certain point of mylonite development, which is probably temperature-determined, GBB is facilitated and the steady-state dynamic recrystallization of clasts sets in. The recrystallized grain size is very close to the grain size in the matrix. Assuming that an inverse proportionality between grain size and stress is valid, the existence of approximate stress homogeneity must be considered in naturally deformed calcite aggregates. A distinct to almost complete dynamic recrystallization of the porphyroclasts and minimum microstructural changes of the matrix indicates significant strain rate differences between the porphyroclasts and the matrix.

- 3) Variscan large-scale thrusting within the Brunovistulian basement is indicated by the juxtaposition of facies with contrasting microstructures which reflect incompatible peak-grade conditions. The main deformational contrasts can be observed between the lower tectonic unit of the Svratka Dome and the other two domains of the Brunovistulicum — the Brno batholith's western margin and the lower tectonic unit of the Thaya Dome.

It seems very likely that the recrystallized grain size within the mylonitized sequence of limestones studied is due to differential stress variations. Assuming this, it is quite surprising that temperature differences probably not exceeding 50 °C resulted in such dramatic changes of differential stresses and responsive microstructures (compare microstructures A and B with D). Actually, we are not the first to have observed indications of such contrasting behaviour of calcite aggregates under natural LT deformation conditions. Burkhard (1990) examined the change of the microfabric of micritic limestones strained under a natural temperature gradient. He found out that up to 250 °C, grain size distributions were indistinguishable from the sedimentary protolith. Above 280 °C, an increase in grain size in micritic limestones occurred along with an increase in the preferred orientation of the lattice and grain-shape. Behrmann (1983) described distinct variations in the microfabric of calcite mylonites strained at about 300 °C. Microstructural features of the tectonofacial succession, which were described above, provide evidence of the dominance of GBB process or nucleation during the progressive part of LT mylonitization. Burkhard (1990) also suggested a grain boundary migration mechanism for grain growth in epizonally strained micrites. Grain boundary migration has a first order dependence on temperature (e.g. Guillopé & Poirier 1979) and it can be expected that the variation of finite microstructures within the limestones strained under LT conditions is due to a significant change of GBB effectiveness at temperatures around 300 °C.

Acknowledgments: We thank the creators of *ImageTool 2.0* for its free provision at <http://www.uthscsa.edu/dig/itdesc.html>. The constructive reviews of K. Schulmann, D. Plašienka and an anonymous reviewer are highly acknowledged. The research was supported by Grant Agency of Czech Republic through Grant No. 205/98/0751 and by research plan J07/98:143100004.

References

- Bábek O. & Janoška M. 1997: Tectonic evolution of the Konice-Mladeč belt: Structural analysis and facies disjunction. *Fac. Rer. Nat., Acta Univ. Palackianae Olomuc., Geol.* 35, 31–35.
- Batik P. & Skoček V. 1981: Lithological development of the Paleozoics in the Thaya Batholith eastern margin. *Věst. ÚÚG* 56, 6, 337–347 (in Czech).
- Behrmann J.H. 1983: Microstructure and fabric transitions in calcite tectonites from the Sierra Alhamilla (Spain). *Geol. Rdsch.* 72, 2, 605–618.
- Bosák P. 1980: Sedimentology of the Devonian in the Tišnov Brunnides and Brno Unit s.s., Tišnov area. *Unpublished PhD. Thesis. Charles University, Prague*, 1–200 (in Czech).
- Bosák P. 1984: Organic matter in the Devonian carbonates of the Tišnov area. *Čas. Mineral. Geol.* 29, 1, 41–53 (in Czech).
- Burkhard M. 1990: Ductile deformation mechanisms in micritic lime-

- stones naturally deformed at low temperatures (150–350 °C). In: Knipe R.J. & Rutter E.H. (Eds.): Deformation mechanisms, rheology and tectonics. *Geol. Soc. Spec. Publ.* 54, 241–257.
- Busch J.P. & Van der Pluijm B.A. 1995: Calcite textures, microstructures and rheological properties of marble mylonites in the Bancroft shear zone, Ontario, Canada. *J. Struct. Geol.* 17, 677–688.
- Casey M. & McGrew A.J. 1999: One-dimensional kinematic model of preferred orientation development. *Tectonophysics* 303, 131–140.
- Cháb J. & Suk M. 1977: Regional metamorphism in Bohemia and Moravia. *Knih. ÚÚG* 50, 156 (in Czech).
- Čížek P. & Tomek C. 1991: Large-scale thin-skinned tectonics in the eastern boundary of the Bohemian Massif. *Tectonics* 10, 273–286.
- Covey-Crump S.J. & Rutter E.H. 1989: Thermally induced grain growth of calcite marbles on Naxos island, Greece. *Contr. Mineral. Petrology* 101, 69–86.
- Dietrich D. & Song H. 1984: Calcite fabrics in natural shear environment, the Helvetic nappes of western Switzerland. *J. Struct. Geol.* 6, 19–32.
- Drury M.R. & Urai J.L. 1990: Deformation-related recrystallization processes. *Tectonophysics* 172, 235–253.
- Dvořák J. 1973: Synsedimentary tectonics of the Paleozoic of the Drahaný Upland (Sudeticum, Moravia, Czechoslovakia). *Tectonophysics* 17, 359–391.
- Dvořák J. 1995: Stratigraphy of the Moravo-Silesian zone. In: Dallmeyer R.D., Franke W. & Weber K. (Eds.): Pre-Permian geology of Central and Eastern Europe. *Springer*, Berlin, 477–489.
- Dudek A. 1980: The crystalline basement block of the outer Carpathians in Moravia — Brunovistulicum. *Rozpr. Čs. Akad. Věd, Ř. Mat. Přír.* 90, 8, 85.
- Finger F., Höck V. & Steyrer H.P. 1989: The granitoids of the Moravian Zone of north-east Austria — Products of a Cadomian active continental margin? *Precambrian Res.* 45, 235–245.
- Finger F., Frasl G., Dudek A., Jelinek E. & Thöni M. 1995: Cadomian Plutonism in the Moravo-Silesian Basement. In: Dallmeyer R.D., Franke W. & Weber K. (Eds.): Pre-Permian geology of Central and Eastern Europe. *Springer*, Berlin, 495–507.
- Finger F., Hanzl P., Pin C., Von Quadt A. & Steyrer H.P. 2000: The Brunovistulian: Avalonian Precambrian sequence at the eastern end of the Central European Variscides? In: Franke W., Haak V., Oncken O. & Tanner D. (Eds.): Orogenic Processes: Quantification and Modelling in the Variscan Belt. *Geol. Soc. London Spec. Publ.* 179, 103–112.
- Francù E., Francù J. & Kalvoda J. 1999: Illite crystallinity and vitrinite reflectance in Paleozoic siliciclastics in the SE Bohemian Massif. *Geol. Carpathica* 50, 5, 365–372.
- Frasl G. 1983: Zur Geologie des Kristallins und Tertiärs der weiteren Umgebung von Eggenburg. Österreichische Geologische Bundesanstalt, *Excursion Guide*.
- Frey M. & Robinson D. (Eds.) 1999: Low-grade metamorphism. *Blackwell Science*, London, 1–313.
- Fritz H., Dallmeyer R.D. & Neubauer F. 1996: Thick-skinned versus thin-skinned thrusting: Rheology controlled thrust propagation in the Variscan collisional belt (The southeastern Bohemian Massif, Czech Republic–Austria). *Tectonics* 15, 6, 1389–1413.
- Fritz H. & Neubauer F. 1993: Kinematics of crustal stacking and dispersion in the southeastern Bohemian Massif. *Geol. Rdsch.* 82, 556–565.
- Guillopé M. & Poirier J.P. 1979: Dynamic recrystallization during creep of single crystalline halite: an experimental study. *J. Geophys. Res.* 84, 5557–5567.
- Hanzl P. & Melichar R. 1997: Brno Massif: a section through the active continental margin or a composed terrane? *Krystalinikum* 23, 33–58.
- Heitzmann P. 1987: Calcite mylonites in the Central Alpine root zone. *Tectonophysics* 135, 207–215.
- Hippert J. & Egydio-Silva M. 1996: New polygonal grains formed by dissolution-redeposition in quartz mylonite. *J. Struct. Geol.* 18, 1345–1352.
- Hirth G. & Tullis J. 1992: Dislocation creep regimes in quartz aggregates. *J. Struct. Geol.* 14, 145–159.
- Jackson M.L. 1975: Soil chemical analysis. Advanced course. Published by the author. *Dept. Soil Sci., Univ. Wisconsin*, Madison, 1–895.
- Jenček V. & Dudek A. 1971: Relationship of the Moravicum and Moldanubicum at the western border of the Dyje Dome. *Věst. ÚÚG* 46, 6, 331–338.
- Kallend J.S., Kocks U.F., Rollet A.D. & Wenk H.R. 1991: Operational Texture Analysis. *Mater. Sci. Engin.*, A132 1–11.
- Kalvoda J. 1995: Devonian sedimentary basins of East Avalonian margin in Moravia. *Geologické výzkumy na Moravě a ve Slezsku v roce 1994*, 48–50 (in Czech).
- Kalvoda J. 2001: Upper Devonian–Lower Carboniferous foraminiferal paleobiogeography and Perigondwana terranes at the Baltica–Gondwana interface. *Geol. Carpathica* 4, 52, 205–215.
- Kohlstedt D.L. & Weathers M. 1980: Deformation-induced microstructures, paleopiezometers, and differential stresses in deeply eroded fault zones. *J. Geophys. Res.* 85, B11, 6269–6285.
- Kübler B. 1967: La crystallinité de l'illite et les zones tout a fait supérieures du métamorphisme. In: Etages Tectoniques, Colloque de Neuchâtel, 1966, *A la Baconnière*, Neuchâtel, 105–122.
- Leichmann J. 1996: Geologie und Petrologie des Brünner Massifs. *Unpublished PhD Thesis, University of Salzburg*.
- Lloyd G.E. & Freeman B. 1994: Dynamic recrystallization of quartz under greenschist conditions. *J. Struct. Geol.* 16, 6, 867–881.
- Matějovská O. 1975: The Moldanubicum gneiss series of southwestern Moravia and its relation to granulites. *Věstník ÚÚG* 50, 345–351.
- Matte P., Maluski H., Rajlich P. & Franke W. 1990: Terrane boundaries in the Bohemian Massif: Result of large-scale Variscan shearing. *Tectonophysics* 177, 151–170.
- Mercier J.C.C., Anderson D.A. & Carter N.L. 1977: Stress in the lithosphere: inferences from steady state flow of rock. *Pure Appl. Geophys.* 115, 199–226.
- Michibayashi K. 1993: Syntectonic development of a strain-independent steady-state grain size during mylonitization. *Tectonophysics* 222, 151–164.
- Morauf W. & Jäger F. 1982: Rb–Sr whole rock ages for Bitesch Gneiss, Moravicum, Austria. *Terra Cognita* 2, 60–61.
- Olgaard D.L. & Evans B. 1988: Grain growth in synthetic marbles with added mica and water. *Contr. Mineral. Petrology* 100, 246–260.
- Rajlich P. 1990: Strain and tectonic styles related to Variscan transpression and transtension in the Moravo-Silesian Culmian basin, Bohemian Massif, Czech Republic. *Tectonophysics* 174, 351–367.
- Ranalli G. 1984: Grain size distribution and flow stress in tectonites. *J. Struct. Geol.* 6, 443–447.
- Rosenholtz J.L. & Smith D.T. 1949: Linear thermal expansion of calcite, var. Iceland spar and Yule marble. *Amer. Mineralogist* 34, 846–854.
- Rutter E.H. 1974: The influence of temperature, strain rate and interstitial water in the experimental deformation of calcite rocks. *Tectonophysics* 22, 311–334.
- Rutter E.H. 1995: Experimental study of the influence of stress, temperature, and strain on the dynamic recrystallization of Carrara marble. *J. Geophys. Res.* 100, 24651–24663.
- Rutter E.H., Casey M. & Burlini L. 1994: Preferred crystallographic orientation development during the plastic and superplastic flow of calcite rocks. *J. Struct. Geol.* 16, 1431–1446.
- Schmid S.M., Boland J.N. & Paterson M.S. 1977: Superplastic flow in finegrained limestone. *Tectonophysics* 43, 257–291.
- Schmid S.M., Paterson M.S. & Boland J.N. 1980: High temperature flow and dynamic recrystallization in Carrara marble. *Tectonophysics* 65, 245–280.
- Schmid S.M., Panozzo R. & Bauer S. 1987: Simple shear experiments on calcite rocks: rheology and microfabric. *J. Struct. Geol.* 9, 747–778.
- Schulmann K., Ledru P., Autran A., Melka R., Lardeaux J.M., Urban M. & Lobkovicz M. 1991: Evolution of nappes in the eastern margin of the Bohemian Massif: a kinematic interpretation. *Geol. Rdsch.* 80/1, 73–92.
- Schulmann K., Melka R., Lobkovicz M., Ledru P., Lardeaux J.M. & Autran A. 1994: Contrasting styles of deformation during progressive nappe stacking at the southeastern margin of the Bohemian Massif (Thaya Dome). *J. Struct. Geol.* 16, 355–370.
- Špaček P. 2001: Microtectonics and stratigraphy of the Paleozoic limestones in the Brunovistulian SW margin. *Unpublished PhD. Thesis, Masaryk University, Brno* (in Czech).

- Štípská P. & Schulmann K. 1995: Inverted metamorphic zonation in a basement-derived nappe sequence, eastern margin of the Bohemian Massif. *Geol. J.* 30, 385–413.
- Stöckhert B., Brix M.R., Kleinschrodt R., Hurford A.J. & Wirth R. 1999: Thermochronometry and microstructures of quartz — a comparison with experimental flow laws and predictions on the temperature of brittle-plastic transition. *J. Struct. Geol.* 21, 351–369.
- Suess F.E. 1908: Die Beziehungen zwischen dem moldanubischen und moravischen Grundgebirge in dem Gebiet von Frain und Geras. *Verh. Geol. Reichsanst.* 393–412.
- Suess F.E. 1912: Die moravischen Fenster und ihre Beziehung zum Grundgebirge des Hohen Gesenks. *Denkschr. K. Akad. Wiss., Wien*, 88, 541–631.
- Suess F.E. 1926: Intrusionstektonik und Wandertektonik im variszischen Grundgebirge. Wien, 268.
- Tullis J. & Yund A. 1982: Grain growth kinetics of quartz and calcite aggregates. *J. Geology* 90, 301–318.
- Twiss R.J. 1977: Theory and applicability of a recrystallized grain-size palaeopiezometer. *Pure Appl. Geophys.* 115, 227–244.
- Ulrich S. 2000: Deformation microstructures and comparative rheology of marble and quartzite in natural strain gradient. *Unpublished PhD. thesis. Charles University, Prague.*
- Van Bremen O., Aflalion A., Bowes D.R., Dudek A., Misař Z., Povondra P. & Vrána S. 1982: Geochronological studies of the Bohemian Massif, Czechoslovakia, and their significance in the evolution of Central Europe. *Transactions of the Royal Society of Edinburgh: Earth Sci.* 73, 89–108.
- Vrána S., Blumel P. & Petrakakis K. 1995: Moldanubian Zone, metamorphic evolution. In: Dallmeyer R.D., Franke W. & Weber K. (Eds.): Pre-Permian geology of Central and Eastern Europe. *Springer, Berlin*, 453–466.
- Walker A.N., Rutter E.H. & Brodie K.H. 1990: Experimental study of grain-size sensitive flow of synthetic, hot-pressed calcite rocks. In: Knipe R.J. & Rutter E.H. (Eds.): Deformation mechanisms, rheology and tectonics. *Geol. Soc. Spec. Publ. No. 54*, 259–284.
- Warr L.N. & Rice H.N. 1994: Interlaboratory standardization and calibration of clay mineral crystallinity and crystallite size data. *J. Metamorphic Geol.* 12, 141–152.
- White S.H. 1977: Geological significance of recovery and recrystallization processes in quartz. *Tectonophysics* 39, 143–170.